Konya Mühendislik Bilimleri Dergisi, c. 12, s. 3, 608-629, 2024
Konya Journal of Engineering Sciences, v. 12, n. 3, 608-629, 2024
ISSN: 2667-8055 (Electronic)
DOI: 10.36306/konjes.1417602

EFFECT OF CHEMICAL MODIFICATION OF MULTIWALL CARBON NANOTUBES ON THE PROPERTIES OF POLY(LACTIC ACID) COMPOSITE FILMS: SYNTHESIS AND CHARACTERIZATION

[1]Figen ARSLAN, [2,*]Şükran Melda ESKİTOROS TOĞAY

[1] Gazi University, Engineering Faculty, Chemical Engineering Department, Ankara, TÜRKİYE
[2] Health Sciences University, Gulhane Vocational School of Health Services, Pharmacy Services Department, Ankara, TÜRKİYE
[1]figen.arslan@hotmail.com, [2]melda.togay@sbu.edu.tr

Highlights

- Unmodified and modified MWCNTs such as MWCNT-COOH, MWCNT-OH, and MA-g-MWCNT were incorporated into the PLA matrix.
- The nanocomposite films were successfully prepared by the solvent casting method.
- These nanocomposite films can be used for different applications due to their improved properties especially in biomedical.

***Corresponding Author:** Şükran Melda ESKİTOROS TOĞAY, melda.togay@sbu.edu.tr

Konya Mühendislik Bilimleri Dergisi, c. 12, s. 3, 608-629, 2024
Konya Journal of Engineering Sciences, v. 12, n. 3, 608-629, 2024
ISSN: 2667-8055 (Electronic)
DOI: 10.36306/konjes.1417602

EFFECT OF CHEMICAL MODIFICATION OF MULTIWALL CARBON NANOTUBES ON THE PROPERTIES OF POLY(LACTIC ACID) COMPOSITE FILMS: SYNTHESIS AND CHARACTERIZATION

[1]Figen ARSLAN, [2,*]Şükran Melda ESKİTOROS TOĞAY

[1] Gazi University, Engineering Faculty, Chemical Engineering Department, Ankara, TÜRKİYE
[2] Health Sciences University, Gulhane Vocational School of Health Services, Pharmacy Services Department, Ankara, TÜRKİYE
[1]figen.arslan@hotmail.com, [2]melda.togay@sbu.edu.tr

(Received: 10.01.2024; Accepted in Revised Form: 21.05.2024)

ABSTRACT: To enhance the properties of poly(lactic acid) (PLA) composite films, unmodified (MWCNT) and modified multiwall carbon nanotubes (MWCNT-COOH, MWCNT-OH, and MA-g-MWCNT) were incorporated into the polymer matrix followed by the solvent casting method. The success of the modification of MWCNT with maleic anhydride (MA) was verified by absorption transmission reflectance spectroscopy (ATR). The fabricated nanocomposite films were analyzed by Fourier transform infrared (FT-IR) spectroscopy, thermal analyses, atomic force microscopy (AFM), contact angle measurements, dynamic mechanical analysis (DMA), and electrical conductivity tests. ATR spectra showed that MA was covalently grafted to the surface of the MWCNT, which was well dispersed and homogenously incorporated in the PLA matrix. The results of the thermal degradation demonstrated that the degradation value of the film increased from 328.91°C to 347°C with the addition of 0.5 wt% MA-g-MWCNT. Additionally, the MWCNT-OH/PLA films illustrated strongly hydrophilic nature due to the –OH groups. The surface resistance of 3 wt% of the MWCNT-COOH/PLA nanocomposite film decreased from 2.56×10^9 to 2.42×10^3 Ω (by 10^6 order). Therefore, the properties of PLA were increased with the addition of functionalized MWCNTs, which can be used for different applications such as biomedical, food packaging, and electronics.

Keywords: *Nanocomposites, Multiwall Carbon Nanotube, Poly(Lactic Acid), Grafting, Maleic Anhydrate*

1. INTRODUCTION

Polymeric nanocomposites have gained much attention due to their significant mechanical, thermal, electrical, and biodegradable properties [1, 2]. Among these nanocomposites, biodegradable polymers have specific properties such as renewable, excellent biodegradable, and biocompatible [3, 4]. Therefore, biodegradable polymeric nanocomposites have been used in almost all areas such as food packaging, biomedical, solar cells, electronic components [5], and eco-friendly applications. These polymers such as poly(lactic acid) (PLA), poly(ethylene oxide) (PEO), poly(3-hydroxybutyrate) (PHB), and polycaprolactone (PCL) [2] have been extensively used in these nanocomposites [1]. Poly(lactic acid) (PLA), which is a biodegradable polyester [6], is derived from renewable resources such as corn and sugar [1]. However, poor mechanical properties, brittleness [7], low crystallization rate, low impact strength, low glass transition temperature, and poor electrical conductivity of PLA severely restrict its applications [4]. Therefore, blending PLA with other polymers or reinforced nanomaterials overcomes these drawbacks of PLA, and leads to the desired properties [8]. To enhance its properties, nanomaterials such as carbon nanotubes [9], montmorillonite [10], and graphene oxide [11] can be used to reinforce.

Multiwall carbon nanotubes (MWCNTs) have attracted a great deal of interest for material sciences due to their high physicochemical properties [12]. MWCNTs possess a large surface area, high elastic modulus, high mechanical and barrier properties, good thermal stability up to 2800°C in a vacuum, and high thermal and electrical conductivity [13]. Thus, they have been used as superior reinforced nanomaterials in polymeric nanocomposites [14]. Especially in the food industry, the studies showed that

***Corresponding Author:** Şükran Melda ESKİTOROS TOĞAY, melda.togay@sbu.edu.tr

there were no harmful effects of the use of MWCNTs as nanofillers [15, 16]. Yu et al. [15] displayed the potential use of grafted MWCNTs in the PHBV films as food packaging. However, the interfacial interaction between polymer matrix and MWCNTs depends on the dispersion of nanofillers in matrices [17]. Seligra et al. [18] developed a technique to disperse MWCNTs in the PLA matrix by linking covalently the nanofiller with the polymer. Yinghui Zhou et al. [19] investigated the effects of the CNTs-COOH nanoparticles on the properties of PLA/CNTs-COOH nanocomposites. The most important issue of the MWCNT nanocomposites is the dispersion of them in the matrix. Therefore, the physical/chemical treatment can be used to improve the dispersion and the compatibility between MWCNT and the polymer matrix [1]. The mechanical performance of the materials can be improved by the strong interfacial adhesion between the matrix and the nanofiller [20] by the functionalization of MWCNT with a compatibilizer agent such as maleic anhydride [21] which is a popular and effective method to enhance this adhesion [22].

To improve the properties of MWCNT, some compatibilizer agents such as maleic anhydride (MA) can be selected. It is highly reactive [23], which enhances the adhesion between polymers and MWNT. MA grafted MWCNT showed better properties than pure MWNT nanoparticles [24]. Huang et al. [24] produced composite materials composed of MA grafted MWCNT and PMMA and investigated the electrical property and EMI shielding efficiency. Wu et al. [25] functionalized MWCNTs with maleic acid (MAA) and maleic anhydride (MA) by the free radical reaction and produced the nanocomposites by the hydrogen bonding with poly (urea urethane) (PUU). Both non-covalent and covalent modifications of the MWCNT surface have been used to improve the wetting and solubility of MWCNT. The advantage of non-covalent attachment is that the perfect structure of the MWCNT is not damaged, and its mechanical properties remain intact. The main disadvantage of this attachment is that the forces between the wrapping molecules and the MWCNT are very weak, which means that the load may not be transferred efficiently from the polymer matrix to the MWCNT filler [26].

Low amounts of MA-g-multi-walled carbon nanotubes (MWCNTs) and other functionalized MWCNT species such as carboxyl (-COOH) and hydroxyl (-OH) groups can indeed act as plasticizers in poly(lactic acid) (PLA) polymer matrices. Here are some literature references that elaborate on this topic specifically in the context of PLA. Zhou et al. [27] described a study where polylactic acid (PLA) was modified with poly(butylene adipate-co-terephthalate) (PBAT) and carbon nanotubes (CNTs-COOH) containing carboxyl groups using melt blending. A compatibilizer, ethylene-butyl acrylate-glycidyl methacrylate (E-BA-GMA), was employed to enhance the interaction between the CNTs-COOH nanoparticles and the PLA/PBAT matrix. The effects of varying CNTs-COOH content on mechanical properties, thermal properties, crystallinity, and morphology of PLA/CNTs-COOH nanocomposites were investigated. The results showed that incorporating CNTs-COOH nanoparticles led to simultaneous improvements in tensile strength, elongation at break, and impact strength of PLA. Additionally, PLA/CNTs-COOH nanocomposites exhibited higher thermal stability compared to pure PLA, with increases observed in glass transition temperature and initial degradation temperature as CNTs-COOH content increased. At low CNTs-COOH content (≤0.5 wt%), the nanoparticles dispersed uniformly in the PLA matrix. Overall, CNTs-COOH were found to be effective fillers for reinforcing and toughening PLA simultaneously, with the PLA/CNTs-COOH nanocomposite containing 0.5 wt% CNTs-COOH demonstrating a favorable combination of strength and toughness [27]. To enhance the performance of PLA (polylactic acid) composites, addressing the poor dispersion and adhesion of carbon nanotubes (CNT) is crucial. Zhang et al. [28] utilized sodium dodecylbenzene sulfonate to modify multi-walled CNT surfaces, improving interfacial adhesion with PLLA (levopolylactic acid) through melt blending. This modification reduced the composite's conductivity below the penetration threshold and enhanced its thermal stability. Additionally, Urtekin et al. [29] leveraged CNT's bridging effect to enhance PLA's interaction with polycarbonate (PC). They compounded variously functionalized multi-walled CNTs (MWCNT, MWCNT-OH, MWCNT-COOH, PC-g-MWCNT) with PC/PLA in a twin-screw extruder. This process facilitated effective grafting of PC onto MWCNT, resulting in improved composite properties. Notably, the addition of 5 wt% MWCNT-OH yielded the highest values for elongation at break, tensile strength, and modulus

in the PC/PLA composites. These studies collectively demonstrate that maleic anhydride-grafted MWCNTs, as well as MWCNTs functionalized with carboxyl and hydroxyl groups, can act as effective plasticizers in PLA polymer matrices, leading to improvements in crystallization behavior, mechanical properties, and thermal stability.

The novelty of this study is that not only the functionalization of MWCNT with MA and also the investigation of the effects of unmodified (MWCNT) and modified multiwall carbon nanotubes (MWCNT-COOH, MWCNT-OH, and MA-g-MWCNT) on the PLA nanocomposites followed by the solvent casting method. Thus, the thermal, mechanical, and electrical properties of nanocomposite materials were determined, and the results of the nanocomposites were compared with neat PLA film.

2. MATERIAL AND METHODS

2.1. Materials

MWCNTs were bought from Timesnano (Chinese Academy of Sciences (CAS)) with a diameter of 10 and 20 nm, a length of 30 μm, and >95 wt% of purity. MWCNT-OH composes of 3.06 wt% -OH content and MWCNT-COOH was 2.00 wt% -COOH content. Poly (L-lactic acid) (PLA) was supplied by Isochem. Chloroform (99%), tetrahydrofuran (99%), acetone (>99%), benzoyl peroxide (BPO) (99%), and maleic anhydride used for functionalization of MWCNTs were purchased from Sigma-Aldrich (St. Louis, USA). All the solvents were used without any further purification.

2.2. Functionalization of the MWCNTs

Maleic anhydride functionalized multiwalled carbon nanotubes (MA-g-MWCNT) were prepared by the following procedure [30]: 1 g of MWCNTs was mixed by refluxing with 2.6 g of maleic anhydride. MA was added into 50 mL of acetone and 50 mL of THF and mixed at 80°C for 4 h. 0.1 g of benzoyl peroxide (BPO) was used as an initiator of the free radical reaction in this procedure. In the last part, anhydrous acetone was used to wash the functionalized MWCNTs (MA-g-MWCNT), and MA-g-MWCNT was centrifuged.

2.3. Preparation of Samples

All the nanocomposite films were prepared by solvent casting method. 5% (w/v) of PLA was added into 100 mL of chloroform and stirred to get a homogenous mixture. Then, appropriate amounts of MWCNT, MWCNT-COOH, MWCNT-OH, and MA-g-MWCNT were separately mixed in this mixture to obtain 0.5, 1, 2, and 3 wt.% ratios of nanofillers. To produce unmodified and modified MWCNT nanocomposites, the solutions were sonicated for 4 h in a water bath at room temperature to enhance the dispersion of MWCNTs and functionalized-MWCNTs in the polymer matrix. The prepared solutions were cast on Petri dishes and put in a vacuum oven at room temperature to remove completely the residue solvent. Finally, the fabricated films were peeled, and the thicknesses were measured as approximately 130 μm. Table 1 shows the amounts of the polymer and nanofillers. 0.5% MWCNT/PLA, 1% MWCNT/PLA, 2% MWCNT/PLA, and 3% MWCNT/PLA nanocomposite films.

Table 1. The prepared polymer solutions for the solution casting method

Films	PLA %	MWCNT %	MWCNT-COOH %	MWCNT-OH %	MA-g-MWCNT %
PLA	5	-	-	-	-
MWCNT/PLA	5	0.5	-	-	-
	5	1.0	-	-	-
	5	2.0	-	-	-
	5	3.0	-	-	-
MWCNT-COOH/ PLA	5	-	0.5	-	-
	5	-	1.0	-	-
	5	-	2.0	-	-
	5	-	3.0	-	-
MWCNT-COOH/PLA	5	-	0.5	-	-
	5	-	1.0	-	-
	5	-	2.0	-	-
	5	-	3.0	-	-
MWCNT-OH/PLA	5	-	-	0.5	-
	5	-	-	1.0	-
	5	-	-	2.0	-
	5	-	-	3.0	-
MA-g-MWCNT /PLA	5	-	-	-	0.5
	5	-	-	-	1.0
	5	-	-	-	2.0
	5	-	-	-	3.0

2.4. Characterization of Samples

2.4.1. ATR spectroscopy

The grafting behavior of the maleic anhydride (MA) onto the MWCNT was analyzed by Absorption Transmission Reflectance (ATR) spectroscopy (Bruker Tensor 27, USA).

2.4.2. FTIR spectroscopy

The chemical bonding of the prepared films was investigated by the Fourier transform infrared (FTIR) spectrometry (Thermo Nicolet Avatar 370 spectrometer, USA). The examination covered a wavenumber range of 4000–400 cm^{-1} with a resolution of 4 cm^{-1} at ambient temperature.

2.4.3. Electrical conductivity

The electrical conductivity was measured using a standard four-point method. All conductivity measurements were determined at room temperature with a Keithley 2400 Source Meter (USA). Rectangular samples of 1 x 5 cm^2 dimensions were prepared for conductivity analysis of the nanocomposite films produced of different types and concentrations. The thickness and resistance values for each sample obtained were taken as the average of the five determined values. The electrical conductivity values of the nanocomposite films were calculated using the resistance values read with the help of the device. The averages of five measurements were reported for each composite.

2.4.4. Thermal characterizations

The thermal gravimetric analysis (TGA) was determined by Pyris 1 TGA device (Perkin Elmer Inc., USA). The samples were heated from 0 to 1000°C under a nitrogen atmosphere with a heating rate of 10°C min^{-1}. In addition, differential scanning calorimeter (DSC) analysis was carried out with the Scinco DSC N-650 instrument (Seoul, Korea). The samples were heated at a temperature range of 25-200°C under a nitrogen atmosphere at an increment of 10°C min^{-1}.
Crystallinity values of the PLA in the nanocomposite films were calculated from the following equation (1):

$$Crystallinity\ (\%) = \left(\frac{\Delta H_m}{93.7}\right) x\ 100 \quad (1)$$

where ΔH_m is the melting enthalpy (J/g) and 93.7 J/g is the theoretical enthalpy of completely crystalline PLA [31].

2.4.5. Contact angle analysis

The surface nature of the materials was evaluated by the water contact angle analysis (WCA) using the Krüss DSA 100 instrument (Hamburg, Germany) at ambient temperature. The measurements involved applying a 5 μL water droplet with the sessile drop method, and the tests were repeated at least three times using deionized water.

2.4.6. Dynamic mechanical analysis

The dynamic mechanical analysis (DMA) was carried out with the Gabo Eplexor 100 N instrument (Germany) in tension mode for a rectangular specimen of dimension (10 x 35 x 2 mm^3). The isochronal frequency of 10 Hz, static load at 1% strain, and dynamic load at 0.2 % strain were applied, and the storage modulus (E'), loss factor (tan δ), and loss modulus (E'') were recorded.

2.4.7. Atomic force microscopy

The atomic force microscopy (AFM) images of 0.5 wt% of the nanocomposite films were obtained using a Park System (XE-100 E instrument, Korea). The analysis covered a 5 × 5 μm^2 area at room temperature, employing a scanning rate of 0.5 Hz and operating in non-tapping mode.

3. RESULTS AND DISCUSSION

3.1. ATR Spectroscopy Analysis

Figure 1 shows the ATR spectra of the MWCNT and the MWCNT functionalized with maleic anhydride (MA), carboxyl (-COOH), and hydroxyl (-OH), respectively.

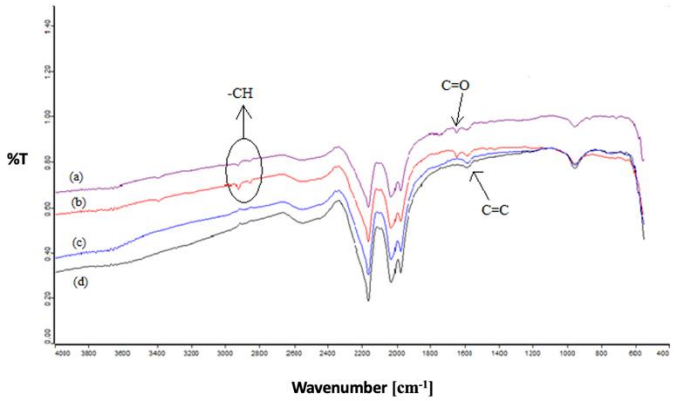

Figure 1. ATR spectrum of nanoparticles (a) MA-g-MWCNT, (b) MWCNT-COOH, (c) MWCNT-OH, (d) MWCNT

The characteristic peak of the aromatic ring (C=C) was obtained between 1600 and 1450 cm^{-1} in the spectra of all the MWCNTs. The stretching vibration of carbonyls (C=O) appeared at 1760-1690 cm^{-1}, which belonged to the carbonyl group (C=O) for MWCNT-COOH and MA-g-MWCNT particles. The C=O stretching at 1721 cm^{-1}, corresponds to the incorporated carboxylic acid groups (-COOH) due to the acid treatment process, characterized the MWCNT-COOH [1]. The C-H stretching at 2853 and 2925 cm^{-1} corresponded to alkyl groups, which comes from the carboxyl group [26]. After the functionalization of MWCNT with maleic anhydride, some organic groups in the chemical structure of maleic anhydride were attached to the surface of MWCNT via the chemical bonds. One of these organic groups, the carbonyl group (C=O), was observed in the spectrum of MA-g-MWCNT at a wavelength of 1740 cm^{-1}. Moreover, the transmittance band appears at 2848 and 2947 cm^{-1} corresponding to alkyl groups (–CH) which is regarding the maleic anhydride [30]. Alkyl groups (-CH) existed in carboxyl acid and maleic anhydride; thus, the stretching frequencies appeared at 2854 cm^{-1} and 2917 cm^{-1}. These peaks were nearly the same for MWCNT-COOH and MA-g-MWCNT.

3.2. FTIR Analysis

The FTIR spectra of nanocomposite films are shown in Figures 2 to 5.

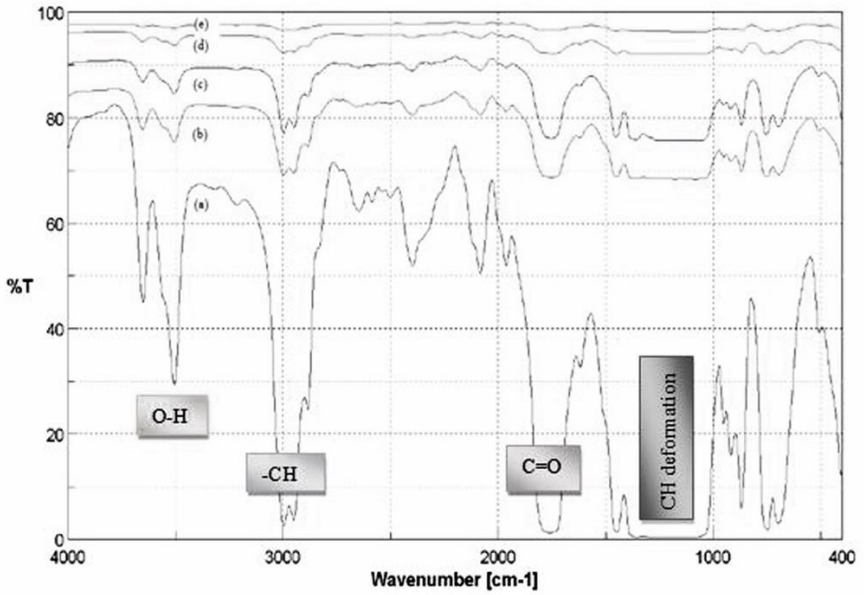

Figure 2. FTIR spectra of (a) neat PLA, (b) 0.5% MWCNT/PLA, (c) 1% MWCNT/PLA, (d) 2% MWCNT/PLA, (e) 3% MWCNT/PLA nanocomposite films

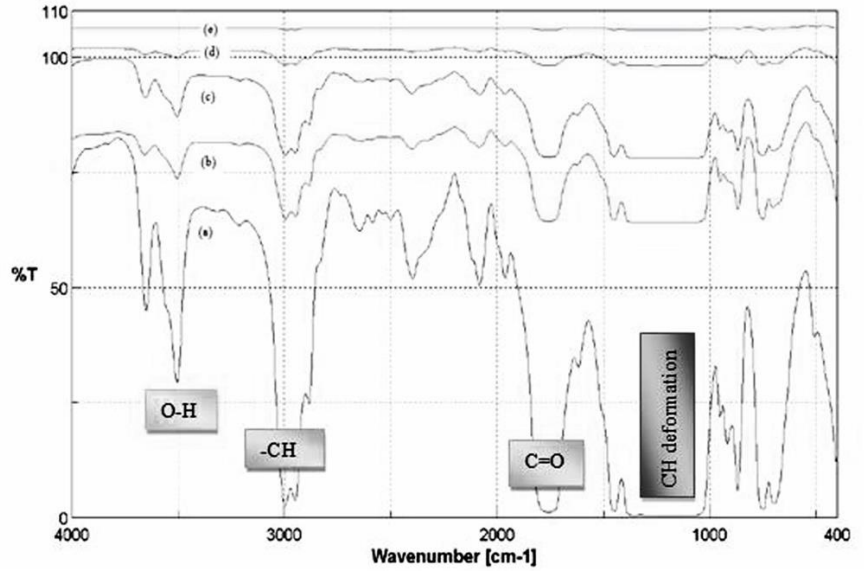

Figure 3. FTIR spectra of (a) neat PLA, (b) 0.5% MWCNT-COOH/PLA, (c) 1% MWCNT-COOH/PLA, (d) 2% MWCNT-COOH/PLA, (e) 3% MWCNT-COOH/PLA nanocomposite films

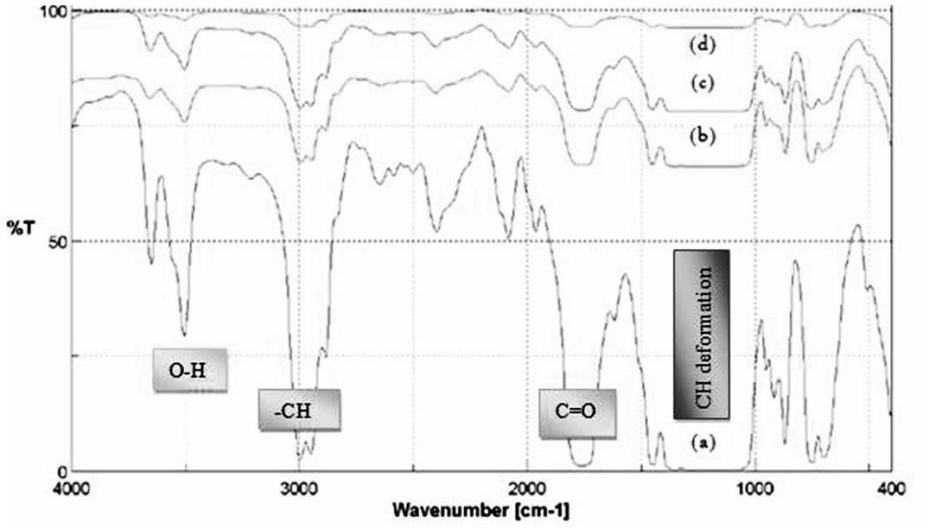

Figure 4. FTIR spectra of (a) neat PLA, (b) 0.5% MA-g-MWCNT/PLA, (c) 1% MA-g-MWCNT/PLA, (d) 2% MA-g-MWCNT/PLA, (e) 3% MA-g-MWCNT/PLA nanocomposite films

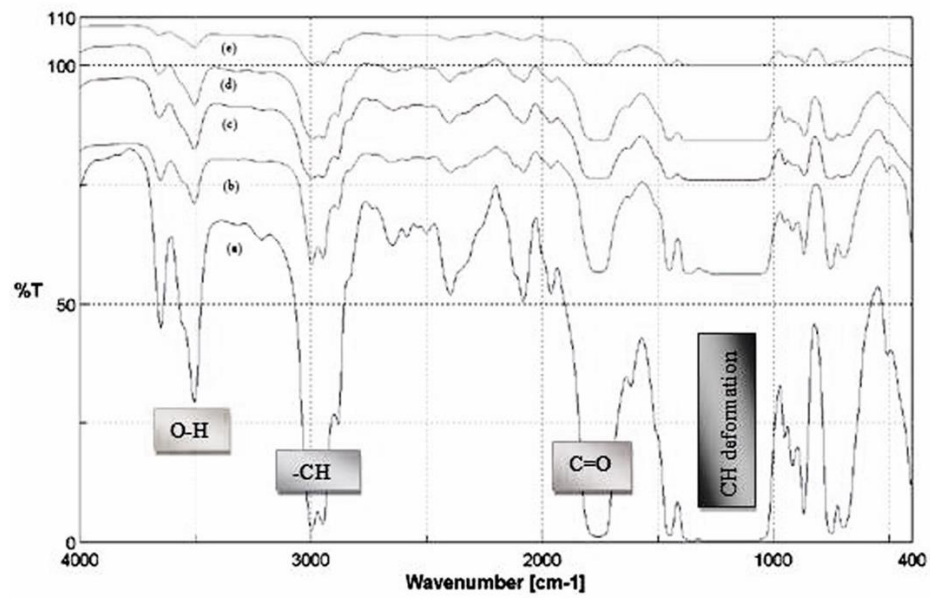

Figure 5. FTIR spectra of (a) neat PLA, (b) 0.5% MWCNT-OH/PLA, (c) 1% MWCNT-OH/PLA, (d) 2% MWCNT-OH/PLA, (e) 3% MWCNT-OH/PLA nanocomposite films

The peaks of pure PLA present CH stretching at 2900-3000 cm^{-1}, C=O carbonyl stretching vibration at 1760 cm^{-1}, CH bending vibrations at 1350-1460 cm^{-1}, and C-C stretching vibration at 870 cm^{-1} [32], as shown in Figures 2 to 5. Accordingly, these peaks were observed for the MWCNT/PLA, MWCNT-COOH/PLA, MA-g-MWCNT/PLA, and MWCNT-OH/PLA nanocomposite films with different amounts of MWCNTs and functionalized MWCNTs. It was clearly understood that when increasing the nanoparticle content of nanocomposite films, the peaks were not observed apparently due to the black color of MWCNT particles. These films were so opaque that they prevented the transmittance of FTIR measurements.

3.3. Electrical Conductivity Analysis

Electrical conductivity relies on the properties of nanofillers such as shape, size, concentration, and distribution of them in the polymer matrix. MWCNTs have a very high aspect ratio in the range of 100-

1000. Therefore, they can build new conductive paths at a low volume fraction [33]. It is well known that chemical functionalization interrupts the extended conjugation of nanotubes, leading to a decrease in the electrical conductivity of functionalized CNTs. Specifically, altering the nanotubes results in a significant reduction in conductivity. Therefore, the electrical conductivity of nanocomposites acquired using functionalized CNT nanoparticles is typically lower compared to those utilizing non-functionalized CNT nanoparticles. On the other hand, some researchers found that the electrical conductivity properties of the types of CNT particles that are functionalized with –COOH or –OH groups may have improved [34]. All the results of the electrical conductivity of the samples were determined by four-point electrical analysis, as shown in Table 2.

Table 2. Electrical conductivity of composites for different types of particles

Particle	Conc., %	R, ohm	ϱ, ohm.cm	σ, ohm.cm^{-1}
-	0	$256*10^{7}$±0.5	$6.8*10^{6}$	$1.47*10^{-7}$
MWCNT	0.5	$132*10^{7}$±0.2	$3.2*10^{6}$	$3.10*10^{-7}$
MWCNT	1	$2.24*10^{7}$±3.5	$4.9*10^{4}$	$2.05*10^{-5}$
MWCNT	2	$6.4*10^{6}$±1.5	$1.3*10^{4}$	$7.96*10^{-5}$
MWCNT	3	2720±0.5	7.18	0.14
MWCNT-COOH	0.5	$6.4*10^{8}$±46.5	$1.9*10^{6}$	$5.08*10^{-7}$
MWCNT-COOH	1	$478*10^{2}$±6.1	182	0.005
MWCNT-COOH	2	4780±0.59	14.9	0.067
MWCNT-COOH	3	2420±0.24	6.1	0.163
MA-g-MWCNT	0.5	$1.6*10^{9}$±0.19	$2.9*10^{6}$	$3.34*10^{-7}$
MA-g-MWCNT	1	$1.2*10^{9}$±0.24	$3.1*10^{6}$	$3.21*10^{-7}$
MA-g-MWCNT	2	$1.9*10^{6}$±0.38	$5*10^{3}$	0.0002
MA-g-MWCNT	3	$8.3*10^{5}$±109.8	$2.3*10^{4}$	0.0004
MWCNT-OH	0.5	$1.5*10^{9}$±0.2	$5.4*10^{6}$	$1.86*10^{-7}$
MWCNT-OH	1	$69*10^{7}$±30.2	$2*10^{6}$	$4.90*10^{-7}$
MWCNT-OH	2	$9.1*10^{4}$±5.5	207.7	0.005
MWCNT-OH	3	$13*10^{3}$±1.6	36.09	0.03

As shown in Table 2, the electrical conductivity of the nanocomposite films was higher than the neat PLA film. In addition, when increased the amount of reinforcements from 0.5% to 3% for MWCNT, MWCNT-COOH, MA-g-MWCNT, and MWCNT-OH in the PLA polymer matrix, the electrical conductivity of the nanocomposite films increased. However, MWCNT-COOH/PLA composite films showed the highest conductivity value. It was observed that the electrical conductivity of the nanocomposite increases with the addition of CNTs to the PLA which has a very low electrical conductivity value due to the π-bonds present in the carbon nanotubes. The carbonyl (C=O) group in the carboxyl (–COOH) group has a π-bond; therefore, the highest increment in electrical conductivity was found in the MWCNT-COOH/PLA composite films.

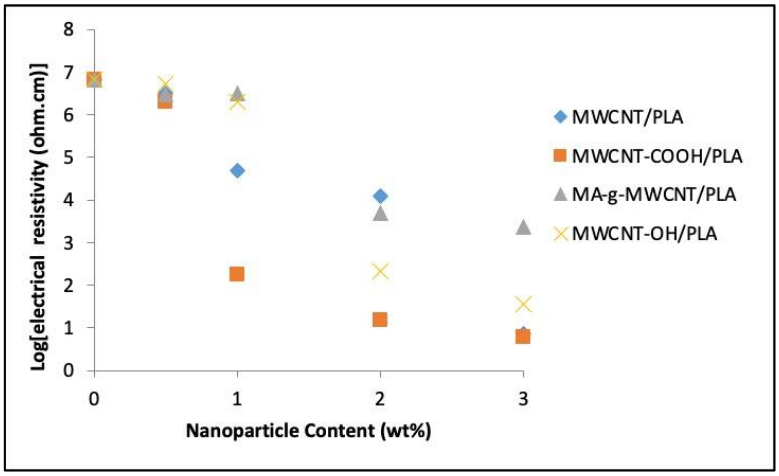

Figure 6. Comparison of electrical resistivity of the composite films

Figure 6 shows the variation of electrical resistivity with respect to the type of nanoparticles. A drastic decrease in the electrical resistivity was obtained at 1 wt.% for the MWCNT-COOH/PLA composite, which indicates that the percolation threshold for the formation of a conductive MWCNT-COOH network in the PLA matrix was reached. Moreover, the percolation threshold was gained at 1.5 wt% for MA-g-MWCNT/PLA and MWCNT-OH/PLA nanocomposites due to decreasing of electrical resistivity.

3.4. Thermal Analysis

Table 3 illustrates the thermal results such as initial thermal degradation temperature, final thermal decomposition temperature, and the percentage of the residue amount. The effect of MWCNT, MWCNT-COOH, MA-g-MWCNT and MWCNT-OH nanoparticles on the thermal degradation temperature and thermal stability of PLA was investigated by TG analysis.

Table 3. The thermal properties obtained by TGA analysis

Films	Conc. of nanoparticle, % wt	Initial decomposition temp, °C	Final decomposition temp, °C	Residue, % at 800°C
Neat PLA	__	328.9	370.3	1.635
MWCNT/PLA	0.5	325.7	371.3	1.531
MWCNT/PLA	1	332.1	371.7	1.820
MWCNT-COOH/PLA	0.5	344.8	377.6	1.986
MWCNT-COOH/PLA	1	343.2	379.2	0.595
MA-g-MWCNT/PLA	0.5	347.0	393.3	0.976
MA-g-MWCNT/PLA	2	340.6	386.7	1.752
MWCNT-OH/PLA	0.5	341.6	377.1	1.986
MWCNT-OH/PLA	2	345.8	378.9	1.492

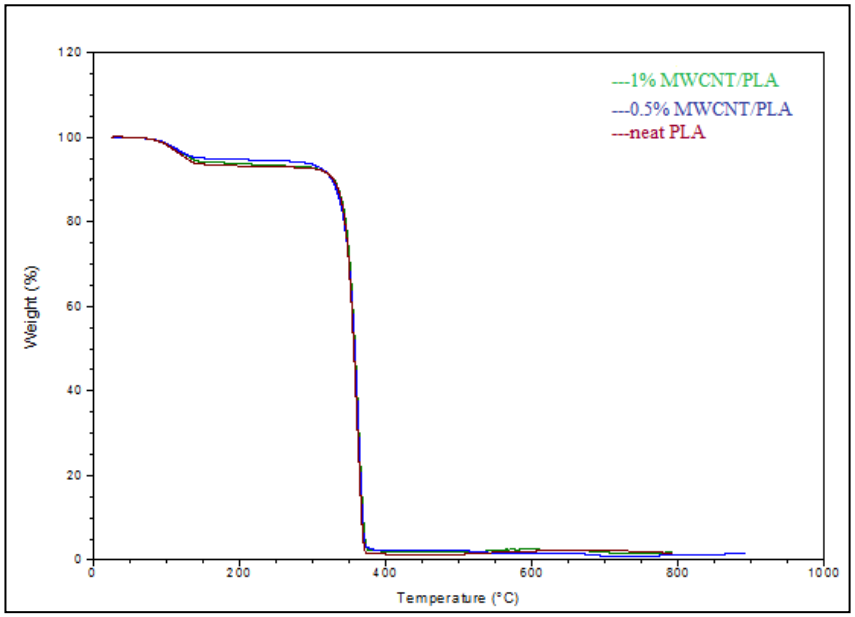

Figure 7. TGA curves of neat PLA, 0.5 wt% MWCNT/PLA and 1 wt% MWCNT/PLA composite films

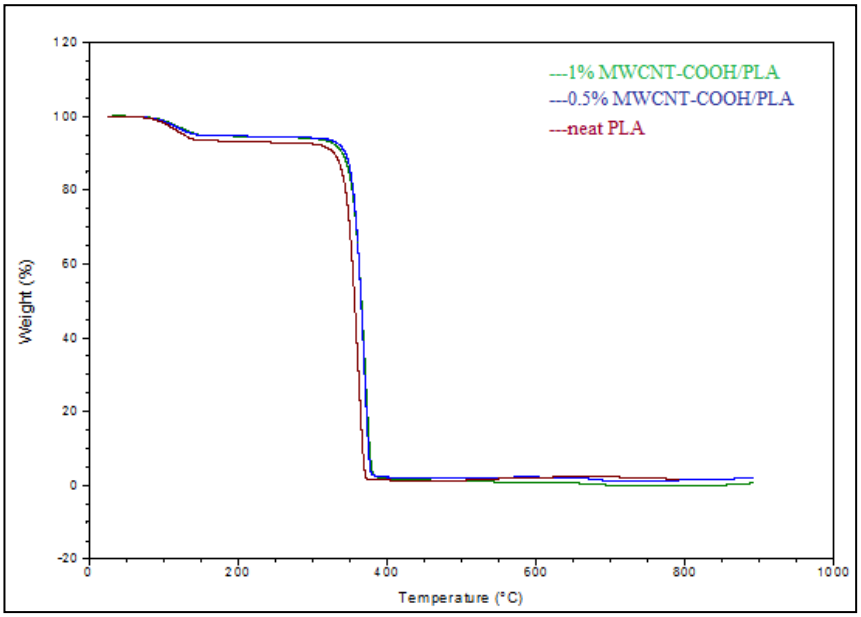

Figure 8. TGA curves of neat PLA, 0.5 wt% MWCNT-COOH/PLA and 1 wt% MWCNT-COOH/PLA composite films

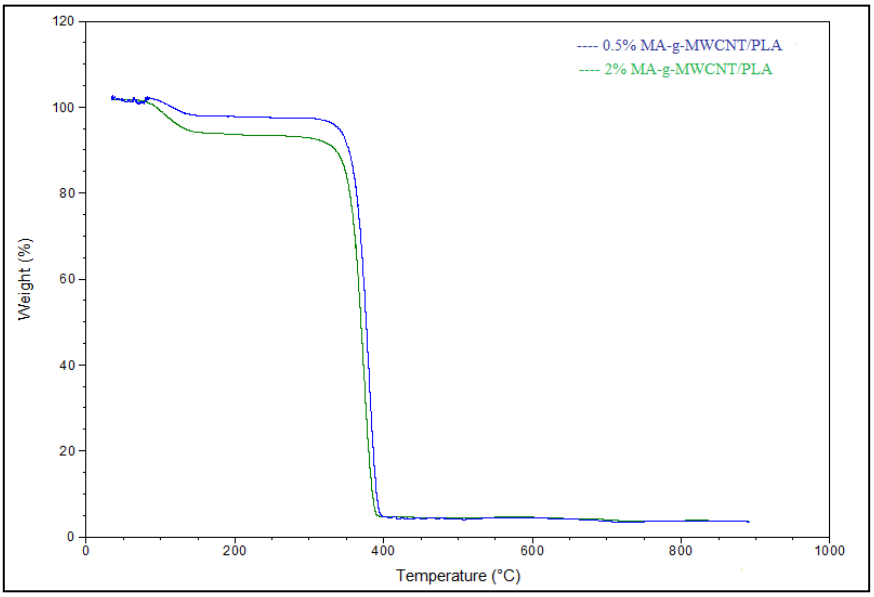

Figure 9. TGA curves of 0.5 wt% MA-g-MWCNT/PLA and 2 wt% MA-g-MWCNT/PLA composite films

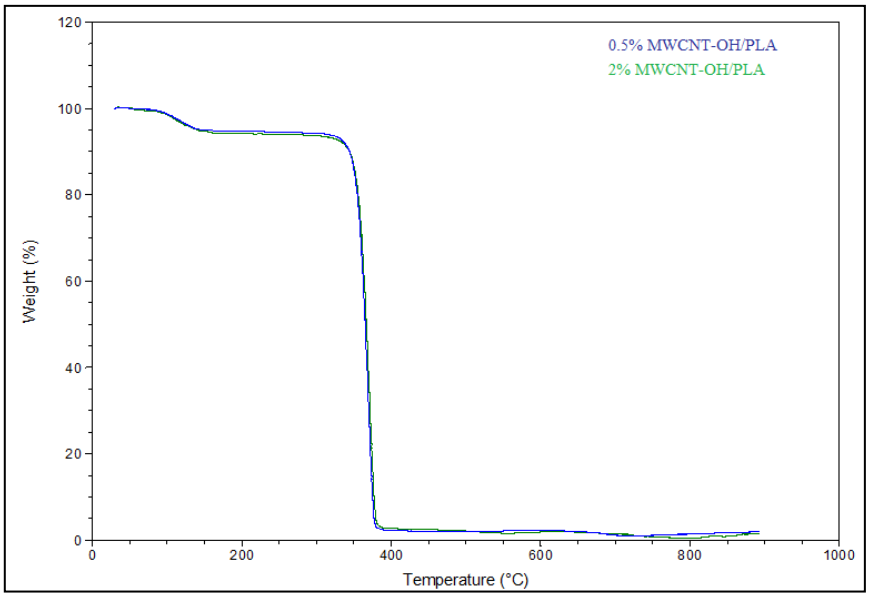

Figure 10. TGA curves of 0.5 wt% MWCNT-OH/PLA and 2 wt% MWCNT-OH/PLA composite films

As can be seen from TGA curves (Figure 7 to 10), the major weight loss was noticed in the temperature range between 300°C and 400°C. The nanocomposite films began to decompose and completed the decomposition at a higher temperature from neat PLA. This condition indicates the improved thermal stability of nanocomposite films due to the high thermal degradation of carbon nanotubes used as a nanofiller. Moreover, the primary purpose of employing a grafting technique is to improve the bonding at the interface between the polymer matrix and MWCNT. This circumstance facilitates efficient transmission of loads from the matrix to the nanoparticle, ultimately boosting thermal stability. As well, the most increment thermal stability of PLA was reached when the addition 0.5 wt% of MA-g-MWCNT with initial decomposition temperature increased from 328.91°C to 347°C due to the better interfacial bond between MA-g-MWCNT and PLA [35]. In the study of Chrissafis [36] on the thermal degradation kinetics of PLA reinforced with MWCNT-COOH and that of Kuan et al. [30] in which PLA polymer was reinforced with carbon nanotubes, the thermal degradation temperatures of nanocomposites were higher than the thermal degradation temperature of pure PLA. When the initial decomposition temperatures of 0.5 wt.% MWCNT-COOH/PLA and 1 wt.% MWCNT-COOH/PLA were compared, the 0.5 wt.% MWCNT-

COOH/PLA nanocomposite film began to decompose at a higher temperature. This is an indication that the addition of MWCNTs-COOH causes a substantial thermal enhancement of PLA, at least at the initial stages of decomposition. This improvement is mainly attributed to good matrix–nanotube interaction, good thermal conductivity of the nanotubes and also due to their barrier effect. The nanocomposite begins to decompose at higher temperatures, although the addition of MWCNTs-COOH seems to have little effect on the temperature which the maximum decomposition rate takes place.

Figure 11 and 12 show the effect of different types of 0.5 wt% and 2 wt% of MWCNTs n nanocomposite films on the glass transition temperature (Tg), melting temperature (Tm), and the melting enthalpy (ΔH_m) obtained by DSC analysis.

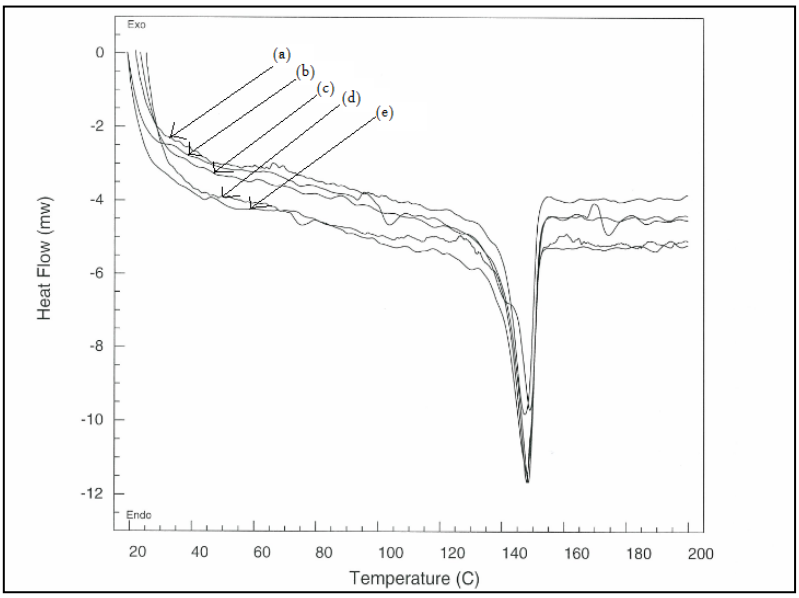

Figure 11. DSC curves of films of (a) 0.5 wt% MWCNT-COOH/PLA, (b) 0.5 wt% MWCNT/PLA, (c) neat PLA, (d) 2 wt% MWCNT/PLA, (e) 2 wt% MWCNT-COOH/PLA

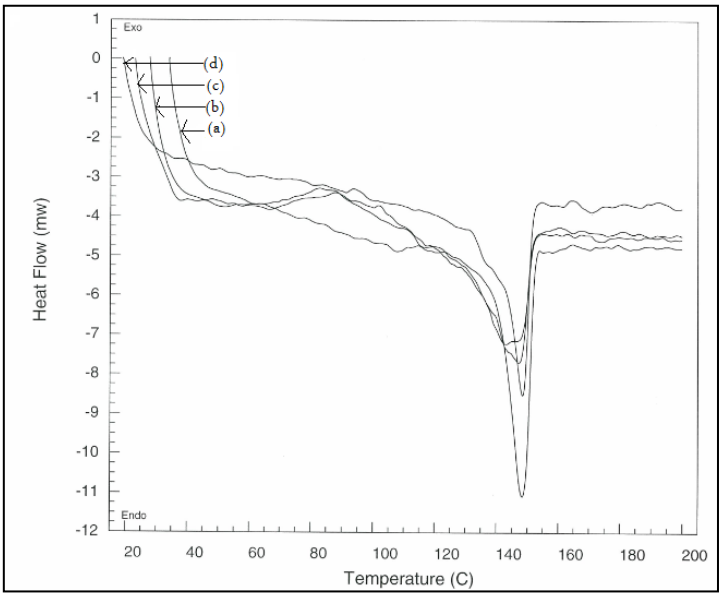

Figure 12. DSC curves of films of (a) 0.5 wt% MA-g-MWCNT/PLA, (b) 2 wt% MA-g-MWCNT/PLA, (c) 0.5 wt% MWCNT-OH/PLA, (d) 2 wt% MWCNT-OH/PLA

The nanocomposite films' glass transition temperature (Tg) is connected to the collective movement of lengthy chain segments, a process that might face obstacles due to MWCNT-OH presence.

Consequently, robust connections between the matrix and the strengthening component might impede the polymer chain's movement, resulting in an elevation in the Tg value [1].

It demonstrated that the Tg increased from 85.78 to 87.74 for the MWCNT-OH/PLA nanocomposite film, and it was higher than neat PLA (Table 4). Therefore, the highest increment was reached with the MWCNT-OH nanofiller. For all the nanocomposite films, when increasing the concentration of nanofillers in the polymer matrix, Tg increased. Conversely, the Tg values were lower than that of neat PLA, unlike MWCNT-OH/PLA nanocomposite film.

Table 4. The thermal properties of neat PLA and the nanocomposite films

Particle	Conc., %	Tg, °C	Tm, °C	ΔH_m, J/g	X_c, %
neat PLA	0	73.7	149.1	28.3	30.2
MWCNT/PLA	0.5	70.6	148.5	31.3	33.4
MWCNT/PLA	2	74.8	148.1	30.9	33.1
MWCNT-COOH/PLA	0.5	66.9	147.4	32.6	34.7
MWCNT-COOH/PLA	2	72.8	148.1	29.6	31.6
MA-g-MWCNT/PLA	0.5	68.6	148.3	32.9	35.2
MA-g-MWCNT/PLA	2	69.5	142.9	37.6	40.1
MWCNT-OH/PLA	0.5	85.8	147.2	46.7	49.8
MWCNT-OH/PLA	2	87.7	148.4	30.8	32.9

Table 3 summarizes the thermal property (Tg, Tm, ΔH_m, Xc) of different types of nanocomposite films. Generally, the melting temperatures (Tm) and melting enthalpy (ΔH_m) decreased with increasing the amount of nanoparticles in the nanocomposite films, and the lowest Tm value was attained at 2 wt% of MA-g-MWCNT/PLA. The Tm values of nanocomposite materials were lower than that of neat PLA. The lowest Tm value was found as 142.96 °C for 2wt% of MA-g-MWCNT/PLA. Wu and Liao [37] explained that the melting temperature (Tm) decreased markedly with an increasing MWNTs–OH content up to 1 wt% and then the effect was slight. The marked decrease in Tm of PLA-g-AA/MWNTs–OH is probably the result of the MWNTs–OH prohibiting the movement of the polymer segments, causing polymer chain arrangement to become more difficult, and also of the hydrophilic character of MWNTs–OH leading to poor adhesion with the hydrophobic PLA.

Moreover, the enthalpy of melting (ΔHm) is a measure of the energy required to melt a material, and it is closely related to the crystallinity of a polymer composite. Higher ΔHm values typically indicate greater crystallinity, as more energy is needed to break the ordered crystalline structure during melting. At 0.5% concentration of the MWCNT/PLA composite film, there was an increase in ΔHm compared to neat PLA, indicating enhanced crystallinity. This suggests that the incorporation of MWCNT improved the crystalline structure of PLA. However, at 2% concentration, ΔHm decreases slightly compared to the 0.5% concentration. This could indicate a saturation effect where higher concentrations of MWCNT might disrupt the crystalline structure, leading to a decrease in crystallinity despite still being higher than neat PLA. For MWCNT-COOH/PLA composites, at both 0.5% and 2% concentrations, ΔHm values are lower compared to neat PLA. This suggests that the presence of MWCNT-COOH may not significantly enhance crystallinity in PLA composites. Both at 0.5% and 2% concentrations of the MA-g-MWCNT/PLA composites, there are substantial increases in ΔHm compared to neat PLA. This indicates that the presence

of MA-g-MWCNT greatly enhances crystallinity in PLA composites, likely due to strong interactions between the grafted MWCNT and the PLA matrix. Additionally, at 0.5% concentration of the MWCNT-OH/PLA composite films, there's a significant increase in ΔHm compared to neat PLA, indicating a substantial enhancement in crystallinity. This suggests that MWCNT-OH effectively promotes crystallization in PLA composites. However, at 2% concentration, ΔHm decreases compared to the 0.5% concentration, which could indicate a disruption in crystalline structure at higher concentrations. Overall, the effects of MWCNT species on crystallinity, as indicated by ΔHm, vary depending on the functional groups and concentrations. While some species enhance crystallinity at certain concentrations, others may exhibit diminishing returns or even disruption of crystalline structure at higher concentrations.

3.5. Dynamic Mechanical Analyzer (DMA)

Figure 13 and Figure 14 depict the mechanical analysis of the neat PLA, 3% MWCNT-COOH/PLA, 3% MA-g-MWCNT/PLA, and 3% MWCNT-OH/PLA samples. It is exactly known that in dynamic mechanical analysis (DMA), the storage modulus (E') and loss modulus (E'') are key parameters used to characterize the mechanical properties of materials over a range of temperatures. The storage modulus (E′) measures the stored energy, relatively the elastic portion of materials. On the other side, the loss modulus (E′′) assesses the energy dissipated as heat, relatively the viscous portion of materials. As well, E′′/E′ ratio gives the tan δ values for DMA analysis.

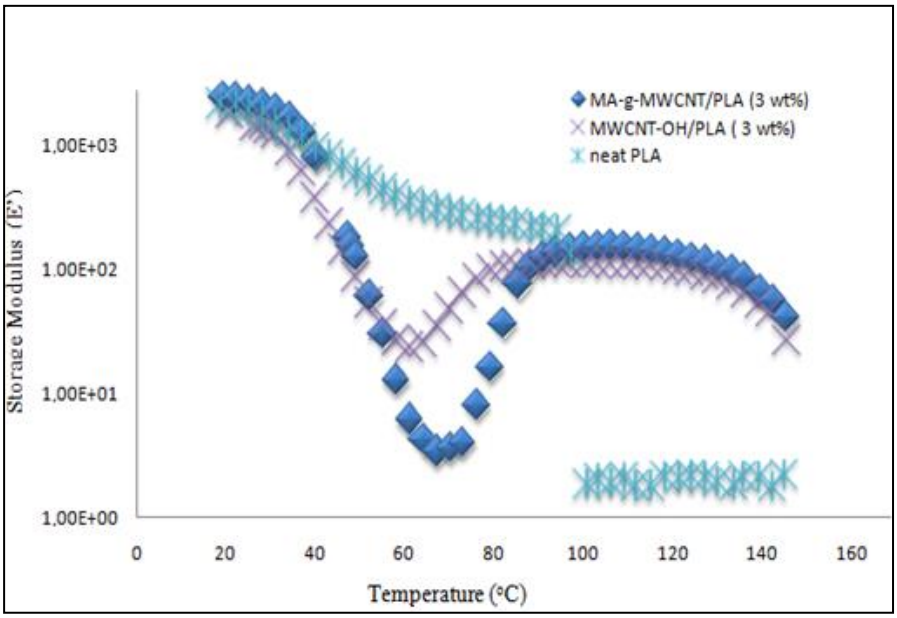

Figure 13. Relationship between the E′ (storage modulus) and temperature

The storage modulus of PLA composites with MA-g-MWCNT showed an increase compared to neat PLA over a certain temperature range. This increase could indicate improved reinforcement effects and better load transfer between the MWCNT and PLA matrix. However, beyond a certain temperature, the storage modulus started to decrease as the material underwent softening or transition to a more viscoelastic state. On the other side, PLA composites with MWCNT-OH exhibited a slight increase in storage modulus compared to neat PLA over a wider temperature range. The presence of hydroxyl functional groups enhanced compatibility between MWCNT-OH and the PLA matrix, leading to improved stiffness and mechanical properties over a broader temperature range.

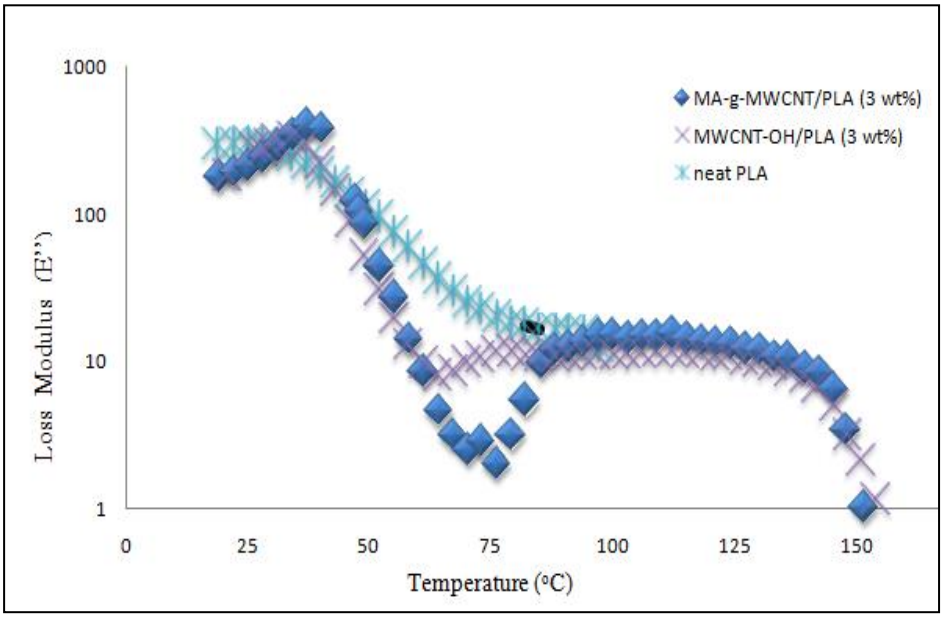

Figure 14. Relationship between the E'' (loss modulus) and temperature

The loss modulus of PLA composites with MA-g-MWCNT increased compared to neat PLA, indicating enhanced damping characteristics. This increase could be due to improved interfacial adhesion and viscoelastic behavior of the composite. Similarly, the loss modulus of PLA composites with MWCNT-OH also increased compared to neat PLA, indicating improved damping characteristics. The enhanced interfacial adhesion and reinforcement effects contribute to the increased loss modulus, especially at higher temperatures.

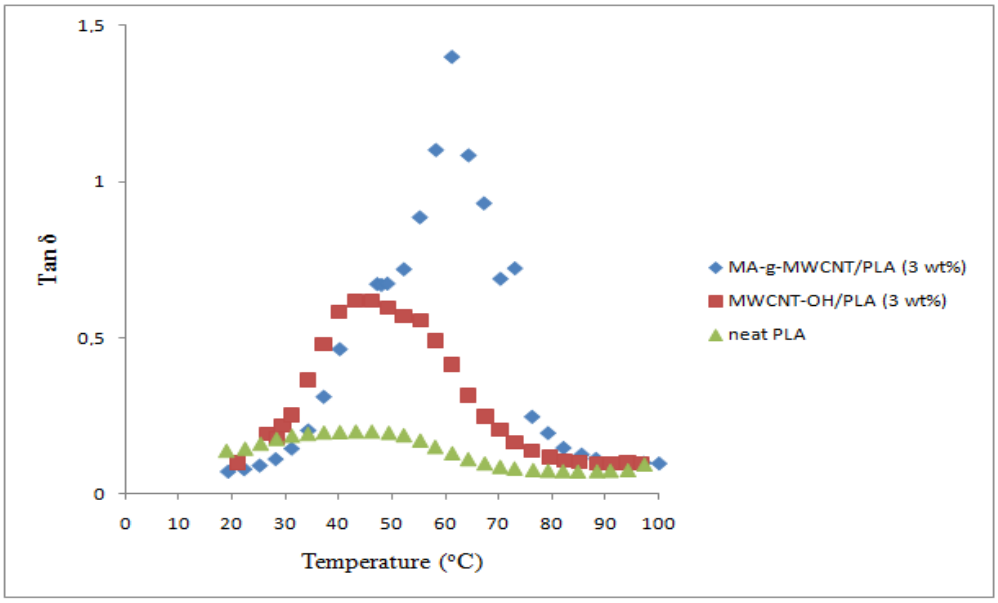

Figure 15. Variation of the tan δ with temperature for MA-g-MWCNT/PLA, MWCNT-OH/PLA and neat PLA

The dynamic mechanical properties of neat PLA and modified-MWCNT/PLA nanocomposites such as MA-g-MWCNT/PLA and MWCNT-OH/PLA including 3 wt% of nanoparticles were measured and determined the compatibility between the matrix and filler. Fig. 15 illustrates variations of the loss tangent (tan δ) with the temperature of the MA-g-MWCNT/PLA, MWCNT-OH/PLA, and neat PLA.

An important observation is that tan δ exhibits a rapid rise at a specific temperature, signifying the

initiation of segmental movement, followed by a subsequent decline.

Overall, the peak becomes wider and less intense as the filler content increases, as the presence of the inorganic network impedes the polymer chains' segmental mobility. The displacement of the tan δ value towards higher temperatures implies the robust interfacial connection between the polymer matrix and the functionalized MWCNT nanoparticles [18]. Relatively, the most efficient bonding obtained in MA-g-MWCNT/PLA nanocomposite with 3 wt% of MA-g-MWCNT due to the shift to high temperature of tan δ value. On the other hand, MWCNT/PLA and MWCNT-COOH/PLA nanocomposite films were very stiff and brittle; therefore, DMA analysis of these nanocomposites couldn't be done.

3.6. Contact angle analysis

Contact angle values for the neat PLA and all the nanocomposite films with concentrations from 0.5 wt% to 3 wt% were given in Figure 16. The water wettability of a material's surface plays a critical role in determining the biological response.

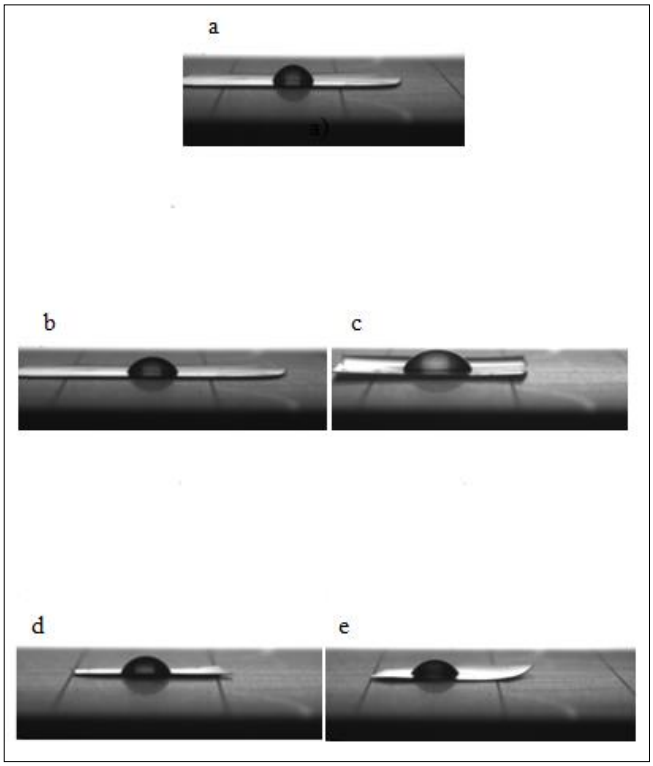

Figure 16. Contact angle images of neat PLA and nanocomposite films (a) neat PLA, (b) MWCNT/PLA, (c) MWCNT-COOH/PLA, (d) MA-g-MWCNT/PLA and (e) MWCNT-OH/PLA

The contact angle value of the neat PLA film was calculated as 82.55°; therefore, PLA is a hydrophobic polymer [1]. After the modification of the surface of MWCNT with -OH group, the contact angle value of the films decreased and this film showed hydrophilic character. Table 5 shows the contact angle values with respect to various concentrations. The results indicated that the MWCNT-OH/PLA films were strongly hydrophilic compared to the other films due to the –OH groups. Moreover, MWCNT/PLA and MA-g-MWCNT/PLA films revealed more hydrophobic character.

Table 5. Contact angle values of neat PLA and its nanocomposite films

Films	Concentration (%)	Contact Angle (°)
Neat PLA	0	82.55 ± 6.72
MWCNT/PLA	0.5	79.65 ± 4.04
MWCNT/PLA	1	80.35 ± 7.06
MWCNT/PLA	2	87.46 ± 0.56
MWCNT/PLA	3	85.75 ± 5.95
MWCNT-COOH/PLA	0.5	79.9 ± 9.0
MWCNT-COOH/PLA	1	77.08 ± 9.30
MWCNT-COOH/PLA	2	70.4 ± 12.40
MWCNT-COOH/PLA	3	71.43 ± 6.64
MA-g-MWCNT/PLA	0.5	82.73 ± 2.03
MA-g-MWCNT/PLA	1	99.28 ± 8.42
MA-g-MWCNT/PLA	2	92.05 ± 13.01
MA-g-MWCNT/PLA	3	84.03 ± 9.41
MWCNT-OH/PLA	0.5	65.93 ± 2.34
MWCNT-OH/PLA	1	62.25 ± 6.25
MWCNT-OH/PLA	2	64.13 ± 2.05
MWCNT-OH/PLA	3	28.55 ± 2.54

3.7. Atomic force microscopy (AFM)

Figure 17 displays AFM images of the neat PLA and its nanocomposite films with the concentration of the nanoparticle of 0.5 wt%.

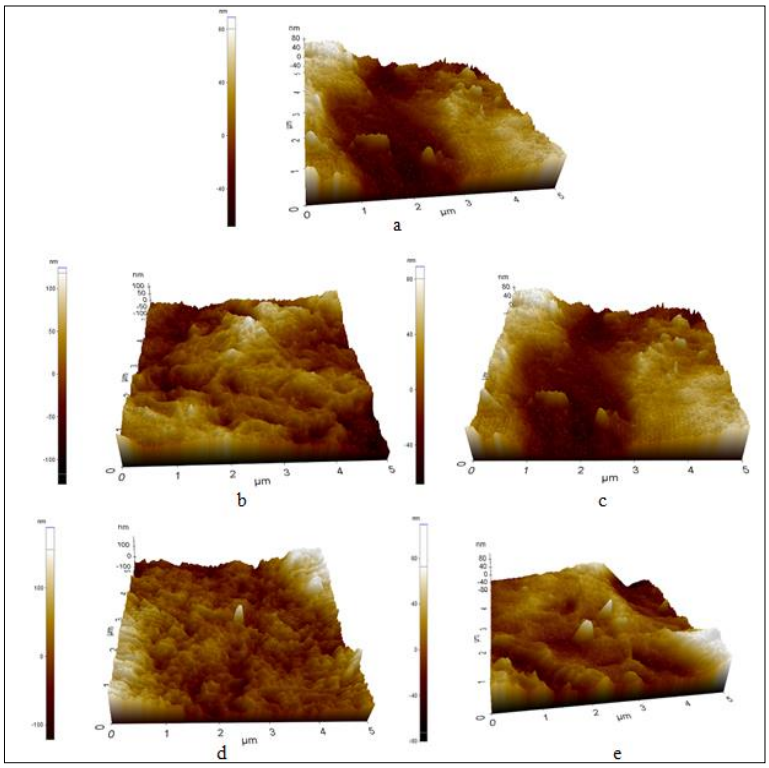

Figure 17. AFM images of neat PLA and its nanocomposite films (a) neat PLA, (b) MWCNT/PLA, (c) MWCNT-COOH/PLA, (d) MA-g-MWCNT/PLA and (e) MWCNT-OH/PLA

As shown in Figure 17, the dispersion of the nanoparticles in the PLA matrix was achieved homogeneously for MA-g-MWCNT/PLA. In Figure 17(b), there was no aggregation in the polymer matrix with MA-g-MWCNT nanoparticles. Therefore, the best interfacial bonding was obtained between the MA-g-MWCNT nanoparticle and PLA.

Table 6. Surface roughness of the neat PLA and its nanocomposite films

Films	Surface roughness value (R_z, nm)
Neat PLA	39.59
MWCNT/PLA	23.15
MWCNT-COOH/PLA	36.12
MWCNT-OH/PLA	20.51
MA-g-MWCNT/PLA	46.47

When the surface roughnesses of the nanocomposite films were compared, the MA-g-MWCNT/PLA films showed the roughest surface at 46.47 nm. While the neat PLA film had a surface roughness of 39.59 nm, it increased to 46.47 for the MA-g-MWCNT/PLA film. The reason is that the roughness increased with the addition of MA-g-MWCNT to the polymer matrix due to the good interaction between the particle and polymer.

4. CONCLUSIONS

The neat PLA and MWCNT/PLA, MWCNT-COOH/PLA, MA-g-MWCNT/PLA, and MWCNT-OH/PLA nanocomposite films were successfully prepared by the solvent casting method. ATR analysis showed that the maleic anhydride (MA) was strongly grafted onto the surface of MWCNT (MA-g-MWCNT). In addition, the dynamic mechanical analysis demonstrated good interfacial adhesion between 3% of the MA-g-MWCNT nanoparticle and the PLA matrix. Thermal analyses represented that the thermal stability of the nanocomposite films increased, and these films completely decomposed at a higher temperature compared to the neat PLA. The most increment of the thermal stability of the films was obtained by the addition of 0.5 wt% MA-g-MWCNT with initial decomposition temperature increased from 328.91°C to 347°C. The surface resistance of the nanocomposite film of 3 wt% MWCNT-COOH/PLA decreased from 2.56×10^9 to 2.42×10^3 Ω (by 10^6 order). Moreover, MWCNT-COOH/PLA composite films illustrated higher electrical conductivity than other nanocomposite films. For AFM analysis, the functionalized MWCNT particles were homogeneously dispersed in the PLA matrix. Consequently, these nanocomposite films can be used for electronic systems, biomedical applications, or as packaging materials due to the improved properties of the PLA polymer with MWCNTs.

Declaration of Ethical Standards

Authors declare to comply with all ethical guidelines including authorship, citation, data reporting, and publishing original research.

Credit Authorship Contribution Statement

F.A: Investigation, Experimental Section, Data Curation, Methodology, Investigation, Writing – original draft. **Ş.M.E.T:** Methodology, Conceptualization, Validation, Resources, Writing – original draft, Writing -review & editing, Supervision.

Declaration of Competing Interest

The authors declare that they have no known competing financial interests or personal relationships that could have appeared to influence the work reported in this paper.

Funding / Acknowledgements

The authors would like to thank Roketsan A.S. for the thermogravimetric analysis.

Data Availability

The data that support the findings of this study are available from the corresponding author upon reasonable request.

5. REFERENCES

[1] C. S. Wu and H. T. Liao, "Study on the preparation and characterization of biodegradable polylactide/multi-walled carbon nanotubes nanocomposites", *Polymer*, vol. 48, no. 15, pp. 4449-4458, 2007.

[2] S. Azizi, M. Azizi, and M. Sabetzadeh, "The role of multiwalled carbon nanotubes in the mechanical, thermal, rheological, and electrical properties of PP/PLA/MWCNTs nanocomposites", *Journal of Composites Science*, vol. 3, no. 3, pp. 64-79, 2019.

[3] R. Scaffaro, F. Lopresti, A. Sutera, L. Botta, R. M. Fontana, and G. Gallo, "Plasma modified PLA electrospun membranes for actinorhodin production intensification in Streptomyces coelicolor immobilized-cell cultivations", *Colloids and Surfaces B: Biointerfaces*, vol. 157, pp. 233-241, 2017.

[4] Y. Zare, H. Garmabi, and K. Y. Rhee, "Structural and phase separation characterization of poly (lactic acid)/poly (ethylene oxide)/carbon nanotube nanocomposites by rheological examinations", *Composites Part B: Engineering*, vol. 144, pp. 1-10, 2018.

[5] H. M. Alghamdi, M. M. Abutalib, A. Rajeh, M. A. Mannaa, O. Nur, and E. M. Abdelrazek, "Effect of the Fe_2O_3/TiO_2 Nanoparticles on the Structural, Mechanical, Electrical Properties and Antibacterial Activity of the Biodegradable Chitosan/Polyvinyl Alcohol Blend for Food Packaging", *Journal of Polymers and the Environment*, vol. 30, no. 9, pp. 3865–3874, 2022.

[6] J. Ahmed and S. K. Varshney, "Polylactides—chemistry, properties and green packaging technology: A review", *International Journal of Food Properties*, vol. 14, no. 1, pp. 37-58, 2011.

[7] J. You, L. Lou, W. Yu, and C. Zhou, "The preparation and crystallization of long chain branching polylactide made by melt radicals reaction", *Journal of Applied Polymer Science*, vol. 129, no. 4, pp. 1959-1970, 2013.

[8] X. Liu, C. Gao, P. Sangwan, L. Yu, and Z. Tong, "Accelerating the degradation of polyolefins through additives and blending", *Journal of Applied Polymer Science*, vol. 131, no. 18, pp. 40750, 2014.

[9] X. Wang, H. Zhou, B. Liu, Z. Du, and H. Li, "Chain extension and foaming behavior of poly (lactic acid) by functionalized multiwalled carbon nanotubes and chain extender", *Advances in Polymer Technology*, vol. 33, no. S1, pp. 21444-21454, 2014.

[10] D. S. Aldana, E. D. Villa, M. Hernández, D. Dios, G. G. Sanchez, Q. R. Cruz, S. F. Gallardo, H. P. Castillo, and L. B. Casarrubias, "Barrier Properties of Polylactic Acid in Cellulose Based Packages Using Montmorillonite as Filler", *Polymers*, vol. 6, pp. 2386-2403, 2014.

[11] B. W. Chieng, N. A. Ibrahim, N. A., W. M. Z. Wan Yunus, M. Z. Hussein, Y. Y. Then, and Y. Y. Loo, "Effects of graphene nanoplatelets and reduced graphene oxide on poly (lactic acid) and plasticized poly (lactic acid): A comparative study", *Polymers*, vol. 6, no. 8, pp. 2232-2246, 2014.

[12] Y. Gogotsi, *Nanotubes and Nanofibers*. Boca Raton, CRC Press, 2006.

[13] B. Kumar, M. Castro, and J. F. Feller, "Poly (lactic acid)–multi-wall carbon nanotube conductive biopolymer nanocomposite vapour sensors", *Sensors and Actuators B: Chemical*, vol. 161, no.1, pp. 621-628, 2012.

[14] S. W. Ko, M. K. Hong, B. J. Park, R. K. Gupta, H. J. Choi, and S. N. Bhattacharya, "Morphological and rheological characterization of multi-walled carbon nanotube/PLA/PBAT blend nanocomposites", *Polymer Bulletin*, vol. 63, pp. 125-134, 2009.

[15] H. Y. Yu, Z. Y. Qin, B. Sun, X. G. Yang, and J. M. Yao, "Reinforcement of transparent poly (3-hydroxybutyrate-co-3-hydroxyvalerate) by incorporation of functionalized carbon nanotubes as a novel bionanocomposite for food packaging", *Composites Science and Technology*, vol. 94, pp. 96-104, 2014.

[16] P. K. Tripathi, S. Durbach, and N. J. Coville, "Synthesis of multi-walled carbon nanotubes from plastic waste using a stainless-steel CVD reactor as catalyst", *Nanomaterials*, vol. 7, no. 10, pp. 284-301, 2017.

[17] N. Thummarungsan, D. Pattavarakorn, and A. Sirivat, "Tuning rigidity and negative electrostriction of multi-walled carbon nanotube filled poly (lactic acid)", *Polymer*, vol. 196, pp. 122488-122499, 2020.

[18] P. G. Seligra, F. Nuevo, M. Lamanna, and L. Famá, "Covalent grafting of carbon nanotubes to PLA in order to improve compatibility", *Composites Part B: Engineering*, vol. 46, pp. 61-68, 2013.

[19] Y. Zhou, L. Lei, B. Yang, J. Li, and J. Ren, "Preparation and characterization of polylactic acid (PLA) carbon nanotube nanocomposites", *Polymer Testing*, vol. 68, pp. 34-38, 2018.

[20] G. E. A. Verginio, T. L. D. A. Montanheiro, L. S. Montagna, J. Marini, and F. R. Passador, "Effectiveness of the preparation of maleic anhydride grafted poly (lactic acid) by reactive processing for poly (lactic acid)/carbon nanotubes nanocomposites", *Journal of Applied Polymer Science*, vol. 138, no. 12, pp. 50087, 2021.

[21] N. F. Braga, H. M. Zaggo, T. L. Montanheiro, and F. R. Passador, "Preparation of maleic anhydride grafted poly (trimethylene terephthalate) (PTT-g-MA) by reactive extrusion processing", *Journal of Manufacturing and Materials Processing*, vol. 3, no. 2, pp. 37, 2019.

[22] Y. Y. Lu, H. Li, and H. Z. Liu, "Maleic anhydride functionalization of multi-walled carbon nanotubes by the electron beam irradiation in the liquid media", *Physica E: Low-dimensional Systems and Nanostructures*, vol. 43, no. 1, pp. 510-514, 2019.

[23] C. Y. Hong, Y. Z. You, and C. Y. Pan, "A new approach to functionalize multi-walled carbon nanotubes by the use of functional polymers", *Polymer*, vol. 47, no. 12, pp. 4300-4309, 2006.

[24] Y. L. Huang, S. M. Yuen, C. C. M. Ma, C. Y. Chuang, K. C. Yu, C. C. Teng, H. W. Tien, Y. C. Chiu, S. Y. Wu, S. H. Liao, and F. B. Weng, "Morphological, electrical, electromagnetic interference (EMI) shielding, and tribological properties of functionalized multi-walled carbon nanotube/poly methyl methacrylate (PMMA) composites", *Composites Science and Technology*, vol. 69, no. 11-12, pp. 1991-1996, 2009.

[25] H. L. Wu, C. H. Wang, C. C. M. Ma, Y. C. Chiu, M. T. Chiang, and C. L. Chiang, "Preparations and properties of maleic acid and maleic anhydride functionalized multiwall carbon nanotube/poly (urea urethane) nanocomposites", *Composites Science and Technology*, vol. 67, no. 9, pp. 1854-1860, 2017.

[26] G. X. Chen, H. S. Kim, B. H. Park, and J. S. Yoon, "Controlled functionalization of multiwalled carbon nanotubes with various molecular-weight poly (L-lactic acid)", *The Journal of Physical Chemistry B*, vol. 109, no. 47, pp. 22237-22243, 2005.

[27] Y. Zhou, L. Lei, B. Yang, J. Li, and J. Ren, "Preparation and characterization of polylactic acid (PLA) carbon nanotube nanocomposites", *Polymer Testing*, vol. 68, pp. 34-38, 2018.

[28] Q. Zhang, H. Quan, J. Liu, D. Gao, and S. Zhang, *China Synthetic Resin and Plastics*, vol. 39, pp. 5, 2022.

[29] G. Urtekin and A. Aytac, "The effects of multi-walled carbon nanotube additives with different functionalities on the properties of polycarbonate/poly (lactic acid) blend", *Journal of Polymer Research*, vol. 28, pp. 1, 2021.

[30] C. F. Kuan, H. C. Kuan, C. C. M. Ma, and C. H. Chen, "Mechanical and electrical properties of multi-wall carbon nanotube/poly (lactic acid) composites", *Journal of Physics and Chemistry of Solids*, vol. 69, no. 5-6, pp. 1395-1398, 2008.

[31] Y. Zare and K. Y. Rhee, "Formulation of tunneling resistance between neighboring carbon nanotubes in polymer nanocomposites", *Engineering Science and Technology, an International Journa*l, vol. 24, no. 3, pp. 605-610, 2021.

[32] N. Nakayama and T. Hayashi, "Preparation and characterization of poly (l-lactic acid)/TiO_2 nanoparticle nanocomposite films with high transparency and efficient photodegradability", *Polymer Degradation and Stability*, vol. 92, no. 7, pp. 1255-1264, 2007.

[33] P. Pötschke, S. M. Dudkin, and I. Alig, "Dielectric spectroscopy on melt processed polycarbonate—multiwalled carbon nanotube composites", *Polymer*, vol. 44, no. 17, pp. 5023-5030, 2003.

[34] N. G. Sahoo, S. Rana, J. W. Cho, L. Li, and S. H. Chan, "Polymer nanocomposites based on functionalized carbon nanotubes", *Progress in Polymer Science*, vol. 35, no. 7, pp. 837-867, 2010.

[35] B. V. Basheer, J. J. George, S. Siengchin, and J. Parameswaranpillai, "Polymer grafted carbon nanotubes—Synthesis, properties, and applications: A review", *Nano-Structures & Nano-Objects*, vol. 22, pp. 100429, 2020.

[36] K. Chrissafis, "Detail kinetic analysis of the thermal decomposition of PLA with oxidized multi-walled carbon nanotubes", *Thermochimica Acta*, vol. 511, no. 1-2, pp. 163-167, 2010.

[37] C. S. Wu and H. T. Liao, "Study on the preparation and characterization of biodegradable polylactide/multi-walled carbon nanotubes nanocomposites", *Polymer*, vol. 48, no. 15, pp. 4449-4458, 2007.